The 2009 IEEE/RSJ International Conference on
Intelligent Robots and Systems
October 11-15, 2009 St. Louis, USA

Real Time Motion Generation and Control for Biped Robot -1st Report: Walking Gait Pattern Generation-

Toru Takenaka, Takashi Matsumoto and Takahide Yoshiike

Abstract—**Generating stable dynamic motions for a biped robot in real time is difficult due to the unstable nature of biped systems and their high degrees of freedom. We propose an approximate dynamics model for biped robots with three masses and no kinematic constraints. We also propose a relaxed boundary condition called "the divergent component of motion". These techniques allow us to generate walking gait patterns with large margin from the edges of support polygon in real time.**

I. Introduction

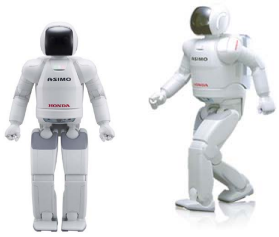

Fig. 1 Walking biped robot system (ASIMO)

For biped robots [1][2] (Fig. 1) to step out of the laboratories and to exist around and collaborate with human, they need abilities to react robustly against unknown events including avoiding collision with previously unknown obstacles and maintaining balance under external disturbances by taking steps. Real time techniques to generate a variety of dynamically stable motions are required to achieve such behaviors.

Zero Moment Point (ZMP) [3] has been used widely as a measure of dynamic balance. ZMP is a point about which the horizontal ground reaction moment of the ground reaction force equals to zero. It can be used to measure instantaneous balance at each time step but does not contain notion of stability in the future. Kajita et al. [4] proposed analytical techniques using linear inverted pendulum model to generate motion for bipeds under real time constraints. Because of the model error, the inverted pendulum quickly diverges from its equilibrium. The technique requires the appropriate design of the ZMP trajectory to prevent the divergence of the upper body trajectory of the biped robot from its equilibrium.

An approach based on the control theory proposed by Kajita et al. [9] designs the position of the center of gravity (CoG) to converge above the position of desired ZMP at the end of the previewing period. Thus, realization of fast motions requires long previewing period. And furthermore, this approach has difficulties in specifying desired ZMP precisely at the heel or toe of the foot to realize human-like walking.

Kajita et al. [4], Nagasaka et al. [5], Kurazume et al. [14], Harada et al. [6], Sugihara et al. [7] and others have proposed approaches which solves boundary value problem, such as desired position and velocity of the CoG, by expressing the desired ZMP trajectory as a function and solving it for general cases. They find necessary modification to the desired ZMP trajectory from the given boundary conditions, and design the CoG trajectory to achieve it. Approaches of Kajita et al. [4] and Kurazume et al. [14] can not specify the time at which the goal state is achieved and can only be applied to walking motions which alternate left and right legs one after another. Nagasaka et al. [5] designed the CoG trajectory which meets the boundary condition as well as minimizes deviation from the original desired ZMP trajectory using quadratic programming. Harada et al. [6] solves for the CoG trajectory while modifying the desired ZMP trajectory as well. These approaches tend to generate large modification from the original desired ZMP trajectories, because the position and the velocity are relatively strict condition. Sugihara et al. [7] proposed to solve this problem by not requiring the continuity of the desired ZMP trajectory and relaxing the boundary conditions so that the position and the velocity of the CoG are not matched at the boundary. However, from our experiences, the real robot tends to lose balance if it tries to follow discontinuous desired ZMP trajectory .

In this paper, we address this problem by decomposing walking motion into two components called the divergent and the convergent components of motion. We relax the boundary condition while satisfying the continuity of the desired ZMP by ignoring the naturally converging component of motion.

Previous approaches to set the upper body trajectory at the end of the gait to come to rest or to certain state heuristically [4][5][6][7][8][14]. It is difficult to set proper boundary conditions for a wide range of pairs of current and next gait patterns. In this paper we use the cyclicity of walking to find the boundary conditions of gait patterns. Yamaguchi et al. [10] also used the cyclic property of walking and generated upper body trajectory in frequency domain to satisfy the desired ZMP trajectory. Park et al. [20] determines the position and velocity of the inverted pendulum from its periodicity as well. Tajima et al. [17] uses the cyclic property of walking-in-place motion and realize walking forward by adding desired forward velocity to it. In this paper, we

Fundamental Research Center, Honda Research & Development, 8-1 Honcho, Wako-shi, Saitama, Japan.

propose an analytical method to design upper body trajectories which converge to a cycle motion gait pattern in infinite time.

Biped robots have heavy mechanical components such as motors in their legs which largely affect their whole body dynamics. A simple linear inverted pendulum model does not account for the legs well and the desired ZMP trajectory designed using it tends to cause problems when the real robot tries to follow it due to the difference in the approximate dynamics. Kajita et al. proposed resolved momentum control [18] and feedback approach using preview control theory [19]. Nishiwaki et al. [8] solved the ZMP equation in discrete time to obtain the upper body motion to compensate for the dynamics error. These approaches need to compute ZMP of the detailed dynamics model by solving inverse kinematics and has computational cost problem as well as having to deal with singularity of the knee joints especially during large acceleration.

Park et al. [20] proposed a model which accounts for the leg dynamics in addition to a linear inverted pendulum. Their model has a point mass near the ankle of each leg to realize small dynamics approximation error. Masses of their ankles have no kinematics constraints to the inverted pendulum. Therefore, that is easy to compute. We extend their model to include inertia terms in addition to the gravity term they have proposed.

In this paper, we use an approximate dynamics model which has two point masses which is kinetically independent from the upper body of the robot to account for the dynamics of the legs in addition to a linear inverted pendulum. Our model has not only small dynamics approximation error and also has low computational cost.

Different from other techniques, gait patterns with large margin from support polygon edge can be generated at every 5 ms.

The remainder of the paper organized as follows. In section II, a general overview of the system is given. In section III, the approximation model of the robot dynamics is introduced. Gait pattern generation is explained and results are shown in section IV and V respectively.

II. System Overview

A gait pattern is a set of trajectories for the desired ZMP, the feet and the upper body.

1. Given a command to move, step position and duration are decided (Fig. 2(a)).
2. Given parameters above, design the desired ZMP and feet trajectories. Then design the upper body trajectory which satisfies the desired ZMP trajectory without causing the upper body to diverge (Fig. 2(b)).
   - 2.1 Generate a gait pattern from a approximate dynamics model using estimate of the future model state (Fig. 2(d)).
   - 2.2 Compensate for the dynamics error due to the approximate dynamics model (Fig. 2(e)).
3. Feed the gait pattern into the real robot, and stabilize it while it is following the gait pattern (Fig. 2(c)).

This paper shows the detail of the walking gait pattern generation process. Extension of the gait generation techniques to running is discussed in [11], the gait pattern modification to compensate approximated dynamics error is discussed in [12] and the integrated balance control is discussed in [13].

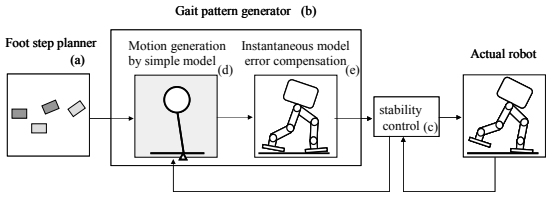

Fig. 2 System overview

III. Approximate Dynamics Model

Because estimating future system state is difficult to do in real time for biped robots due to their highly non-linear dynamics and kinematic constraints, we use the following approximate dynamics model instead of the detailed dynamics model.

A. Three Mass Model

The following properties are desired for approximate dynamics biped robot models.

1. Dynamics difference between the approximate dynamics model and real robot is adequately small.
2. Computation cost of the dynamics using the model is small.

Considering these, we use a three mass model which consists of an inverted pendulum and two foot masses as shown in Fig. 3. Our model has following properties.

1. The model has three point masses, one mass at the end of the inverted pendulum, another at the ankle of the support leg and another at the ankle of the swing leg.
2. There is no kinamtic constraints between the feet and the inverted pendulum to reduce computational complexity.
3. Values of the three masses are designed to match the static and dynamic properties of the real robot. For example, the leg mass of the real robot is distributed to both pendulum mass and foot mass.
4. The height of the pendulum is fixed at some distance from the ground and the pendulum undergoes linearized dynamics.
5. Motions in the sagittal and frontal planes are decoupled. In this paper, motion on the frontal plane is not discussed for simplicity.

The model has only three masses so that kinematic constraints can be ignored. If knee mass is added, for example, one needs to consider kinematic constraints as well as singularity. The variables describing the approximate dynamics model are as follows.

$m_{\mathrm{sup}}, m_{swg}$: The foot mass of the support and swing leg.

m_{pend} : The mass of the inverted pendulum.

m_{total} : The total mass of the dynamics model ($= m_{pend} + m_{\sup} + m_{swg}$).

m_{feet} : Sum of each foot mass. ($= m_{\sup} + m_{swg}$).

x_{pend} : The horizontal position of the end of the inverted pendulum model, on the real robot, this corresponds to the upper body position.

$x_{\sup}, z_{\sup}$: The horizontal and vertical position of the foot mass on the support leg.

x_{swg}, z_{swg} : The horizontal and vertical position of the foot mass on the swing leg.

h : The height of the inverted pendulum (constant).

x_{pend}^{ZMP} : The ZMP of the inverted pendulum.

x_{cog}, z_{cog} : The horizontal and vertical position of the CoG.

g : The gravitational constant.

x_{total}^{ZMP} : The total ZMP of the model.

The origin of coordinate frame is located at the vertical projection of the ankle of the support leg onto the ground when its sole is in full contact with it. This coordinate frame is referred to as the support leg coordinate frame, and through the rest of the paper, quantities are expressed in this coordinate frame unless otherwise noted. Note that torque is expressed about point P on the ground which is located at x_p, z_p .

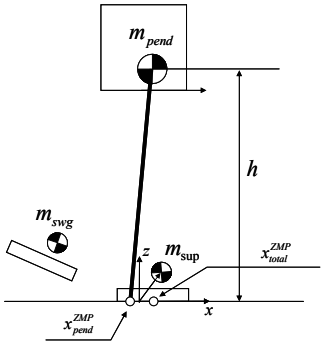

Fig. 3 Dynamics model with three masses

The ground reaction moment about point P due to the feet masses is called the feet moment M_{feet}.

$$\begin{aligned} M_{feet} = {} & m_{\sup}(x_{\sup} - x_p)(g + \ddot{z}_{\sup}) \\ & - m_{\sup}(\ddot{x}_{\sup})(z_{\sup} - z_p) \\ & + m_{swg}(x_{swg} - x_p)(g + \ddot{z}_{swg}) \\ & - m_{swg}(\ddot{x}_{swg})(z_{swg} - z_p) \end{aligned} \quad (1)$$

The ground reaction moment about point P due to the pendulum mass is called the pendulum moment M_{pend}, and can be expressed using the horizontal position of the inverted pendulum as follows.

$$M_{pend} = m_{pend}\, g(x_{pend}^{ZMP} - x_p) \quad (2)$$

The total ground reaction moment due to the three mass model is M_{total}.

$$M_{total} = M_{feet} + M_{pend} \quad (3)$$

And M_{total} is related to x_{total}^{ZMP} as follows

$$M_{total} = m_{total}(x_{total}^{ZMP} - x_p)(g + \ddot{z}_{cog}) \quad (4)$$

Assuming small vertical acceleration of the CoG for walking,

$$\ddot{z}_{cog} << g \quad (5)$$

the following approximation is true.

$$M_{total} = m_{total} g(x_{total}^{ZMP} - x_p) \quad (6)$$

From Eq. (2)(6), we define x_{feet}^{ZMP}

$$M_{feet} = m_{feet} g(x_{feet}^{ZMP} - x_p) \quad (7)$$

Note that x_{feet}^{ZMP} in Eq. (7) is not the same as the point where the moment due to foot masses and gravitational force cancel out to 0. From Eq. (2)(3)(6)(7),

$$x_{pend}^{ZMP} = \frac{m_{total}}{m_{pend}} x_{total}^{ZMP} - \frac{m_{feet}}{m_{pend}} x_{feet}^{ZMP} \quad (8)$$

Eq. (8) is largely affected by the choice of point P because Eq. (5) generates ZMP error proportional to $(x_{total}^{ZMP} - x_p)$. Thus, point P is placed at x_{total}^{ZMP} .

The following is true for the inverted pendulum

$$\ddot{x}_{pend} = \frac{g}{h}(x_{pend} - x_{pend}^{ZMP}) \quad (9)$$

Using Eq. (8), the desired trajectory of the upper body as follows.

1) Given gait parameters, compute a desired x_{total}^{ZMP} trajectory and feet trajectory.
2) Place point P at the desired x_{total}^{ZMP} .
3) Compute M_{feet} from Eq. (1).
4) Compute x_{feet}^{ZMP} from Eq. (7).
5) Substitute the desired x_{total}^{ZMP} and x_{feet}^{ZMP} into Eq. (8) to obtain x_{pend}^{ZMP} .
6) Compute acceleration of the inverted pendulum from Eq. (9) and integrate it to obtain its horizontal velocity and position. This is the upper body motion on the real robot.

B. The Convergent and Divergent Components of Motion

To generate current gait pattern of the inverted pendulum of the three mass model, its conditions at the end of current gait pattern need to be specified. Instead of position and velocity which are commonly used boundary conditions, we propose to use another condition which we call the divergent component of motion. We decompose motions of the inverted pendulum into convergent and divergent components, and show that modification to the ZMP can be decreased by only controlling the divergent component. We also show that by writing the desired ZMP trajectory as a series of straight lines, the required modification to the desired ZMP trajectory to match the boundary condition can be solved analytically.

The linear inverted pendulum follows the dynamics described in Eq. (9) and has the following natural frequency ω_0.

$$\omega_0 = \sqrt{g / h} \quad (10)$$

Now we define p and q as follows.

$$\begin{pmatrix} p \\ q \end{pmatrix} = \begin{pmatrix} 1 & -1/\omega_0 \\ 1 & 1/\omega_0 \end{pmatrix} \begin{pmatrix} x_{pend} \\ \dot{x}_{pend} \end{pmatrix} \quad (11)$$

Using p and q, Eq(9) can be transformed to

$$\frac{d}{dt}\begin{pmatrix} p \\ q \end{pmatrix} = \begin{pmatrix} -\omega_0 & 0 \\ 0 & \omega_0 \end{pmatrix} \begin{pmatrix} p \\ q \end{pmatrix} + \begin{pmatrix} \omega_0 \\ -\omega_0 \end{pmatrix} x_{pend}^{ZMP} \quad (12)$$

where x_{pend}^{ZMP} is given by Eq. (8). If x_{pend}^{ZMP} equals 0,

$$\begin{pmatrix} p \\ q \end{pmatrix} = \begin{pmatrix} C_1 e^{-\omega_0 t} \\ C_2 e^{\omega_0 t} \end{pmatrix} \quad (13)$$

where C_1 and C_2 are arbitrary constants. When x_{pend}^{ZMP} becomes a constant C, p converges to C and q diverges with a time constant of $1/\omega_0$. Because of its naturally converging property, the convergent component is guaranteed to converge without being controlled. Thus only the divergent component needs be considered as a boundary condition when generating a gait pattern.

From Eq. (8)(12) the diverging component at time t, $q(t)$, can be written as follows.

$$q(t) = e^{\omega_0 t} q(0) - \frac{m_{total}}{m_{pend}} \int_0^t e^{\omega_0 (t-\tau)} \omega_0 x_{total}^{ZMP} d\tau + \frac{m_{feet}}{m_{pend}} \int_0^t e^{\omega_0 (t-\tau)} \omega_0 x_{feet}^{ZMP} d\tau \quad (14)$$

Eq. (14) consists of the initial value term, the desired ZMP term and the feet ZMP term. The second and third terms can be computed from the desired ZMP and the feet ZMP. The feet ZMP can be computed by combining the feet trajectory and Eq. (1)(7).

C. The ZMP Trajectory and the Divergent Component

Here, we design desired ZMP trajectory as a sequence of straight lines so that the desired ZMP term in Eq. (14) can be solved analytically.

Let a rectangle of height 1 and width T represent the desired ZMP between time 0 and T (Fig. 4, left). Using this, the second term of the right hand side of Eq. (14) becomes

$$U(T) = \frac{m_{total}}{m_{pend}} (1 - e^{\omega_0 T}) \quad (15)$$

Similarly, let a straight line with slope 1/T and no offset be the desired ZMP between time 0 and T (Fig. 4, right). Using this, the second term of the right hand side of Eq. (14) becomes

$$R(T) = -\frac{m_{total}}{m_{pend}} \left(\frac{1 - e^{\omega_0 T}}{T} + \omega_0\right) \quad (16)$$

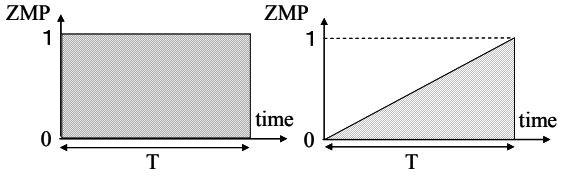

Fig. 4 ZMP trajectory basis

Fig. 5 is an example of the desired ZMP trajectory as a series of straight lines. The gait starts at time 0 and ends at time t_E. The trajectory is divided into intervals, and interval j starts at time t_j and the desired ZMP is $x_{total(j)}^{ZMP}$. The area under the desired ZMP of each interval consists of a rectangle region(Fig. 5, area A) and a triangle region (Fig. 5, area B).

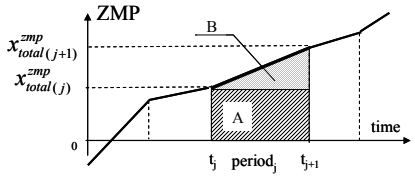

Fig. 5 Example ZMP trajectory

The following is the divergent component at the end of the current gait due to the jth interval.

$$q_j^{ZMP} = e^{\omega_0 (t_E - t_{j+1})} \{ x_{total(j)}^{ZMP} U(t_{j+1} - t_j) + \frac{x_{total(j+1)}^{ZMP} - x_{total(j)}^{ZMP}}{t_{j+1} - t_j} R(t_{j+1} - t_j) \} \quad (17)$$

Summing over all intervals,

$$q^{ZMP} = \sum_{j=0} q_j^{ZMP} \quad (18)$$

Using Eq. (18), the divergent component resulting from a given desired ZMP trajectory can be computed analytically. Then Eq. (14) at time t_E is

$$q(t_E) = e^{\omega_0 t_E} q(0) + q^{ZMP} + \frac{m_{feet}}{m_{pend}} \int_0^{t_E} e^{\omega_0 (t-\tau)} \omega_0 x_{feet}^{ZMP} d\tau \quad (19)$$

IV. Gait Pattern Generation

A. Flow of Gait Pattern Generation

Fig. 6 shows the flow of generating a gait pattern. Once a command is given (a), the feet trajectory of the current and the next cyclic gaits are determined (b). The relative position and velocity of the two legs at the end of the cycle coincide with those at the beginning of the cycle. The desired ZMP trajectories for the current gait and the next cyclic gait are determined (c). The next gait pattern is always cyclic meaning that its initial and terminal states are identical(Fig.7). And the current gait is modified so that its terminal state equals the initial state of the next cyclic gait.

Here the desired ZMP trajectories are designed such that it is at the heel of the foot at the beginning of single support phases, and go though the center of the support polygon to have a large region of stability, then leave the toe at the end of the single support phases. Each of single and double phases is divided into subintervals and a straight line is designed for each subinterval (Fig. 8).

After the leg and the desired ZMP trajectories are determined, the divergent component at the beginning of the cyclic gait is

computed (d). Then the divergent component at the end of the cyclic gait is computed as well as the difference from (e).
The desired ZMP trajectory of the current gait is modified so that the divergent component of the current gait matches with that of the next cyclic gait at the boundary (f).
The desired ZMP trajectory and feet ZMP trajectory are substituted into Eq. (8)(9) to obtain the position of the inverted pendulum. Then desired angle is obtained by solving inverse kinematics.

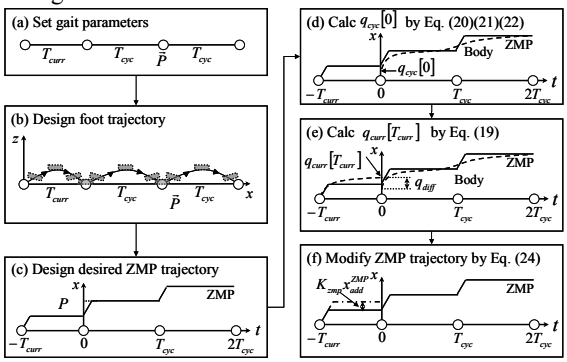

Fig. 6 Flow of gait pattern generation

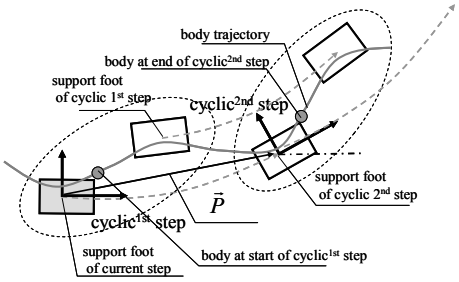

Fig. 7 Cyclic gait coordinate system

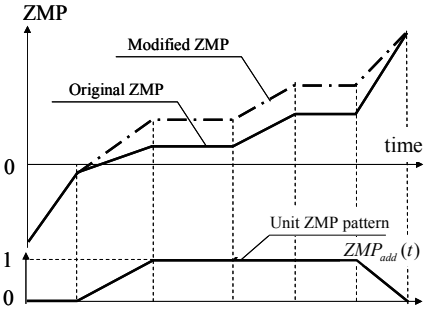

Fig. 8 Modifying ZMP trajectory

B. The Divergent Component of a Cyclic Gait

In case a switch to another gait pattern at the end of the current gait is requested, the current gait is modified such that the initial conditions of the next gait pattern are met at the end of the current gait. Note that, as long as the same gait pattern is used, it can be used without modification to continue walking due to the design of our gait patterns.
To realize gait pattern with direction changes, our cyclic gait consists of two steps (Fig. 7). The first cyclic step in the current support leg coordinate frame and the second swing leg in the second support leg of the cyclic gait pattern coordinate frame coincide. Thus once the positions of current step and the first step of the next cyclic gait are determined, the landing position of the second step of the cyclic gait is determined.
The divergent component, defined and explained in the previous section, is used as the boundary condition of a cyclic gait pattern. In this paper, we limit the discussions to gait patterns for walking straight for simplicity.
T_{curr} : The period of one step of the current gait.
T_{cyc} : The period of one step of the next gait.
$\vec{P}$: The ground contact position of the second support leg with respect to the ground contact position of the support leg of the current gait.
$q_{cyc}(t)$: The divergent component of the cyclic gait at time t
t : The time from the beginning of the cyclic gait.
The coordinate frame defined at the ground contact position of the second support leg of the cyclic gait is referred to as the second coordinate frame.

$$q_{cyc}^{coord2}(T_{cyc}) = q_{cyc}(T_{cyc}) - \vec{P} \tag{20}$$

From Eq. (19), the following is derived.

$$q_{cyc}(T_{cyc}) = e^{\omega_0 T_{cyc}} q_{cyc}(0) + q_{cyc}^{ZMP} + q_{cyc}^{feet} \tag{21}$$

The second and third terms of the right hand side of Eq. (21) correspond to those at Eq. (19) respectively. The relative position of the upper body with respect to the ground contact point of the support leg at the end of the cyclic gait pattern is the same as that at the beginning by our definition of a cyclic gait pattern. Thus,

$$q_{cyc}^{coord2}(T_{cyc}) = q_{cyc}(0) \tag{22}$$

and Eq. (20)-(22) can be solved for $q_{cyc}(0)$.

C. Satisfying the Divergent Component Condition

The desired ZMP trajectory of the current gait is modified so that the divergent component becomes $q_{cyc}(0)$ at the end of the current gait. From the feet trajectory and the desired ZMP trajectory of the current gait, the divergent component $q_{curr}(T_{curr})$ can be computed using Eq. (19). We define q_{diff} as follows.

$$q_{diff} = q_{cyc}(0) - q_{curr}(T_{curr}) \tag{23}$$

A trapezoid of unit height, $ZMP_{add}(t)$ shown in Fig. 8, is used to modify the current desired ZMP trajectory. The side and the top vertices of the trapezoid correspond to a line segment of the desired ZMP trajectory. q_{unit} , the divergent component generated due to the trapezoid, can be computed from Eq. (18). K_{zmp} , the ratio of q_{unit} to q_{diff} is computed as follows.

$$K_{zmp} = q_{diff} / q_{unit} \tag{24}$$

Setting the height of $x_{add}^{ZMP}(t)$ to K_{zmp} and adding it to the current desired ZMP trajectory, a new desired trajectory satisfying the boundary condition is obtained.
Note that at least two degrees of freedom are required to satisfy two boundary conditions, such as position and

velocity, simultaneously. This tends to cause a large modification to the originally designed ZMP trajectory. On the other hand, the divergent component is one condition, and the ZMP modification tends to be small. This decreases the chance that the modified ZMP goes out of the support polygon under fast motions. See appendix for why the ZMP modification is minimized using divergent component as the boundary conditions.

If the commanded walking parameters such as step position and duration are not properly set, the modified ZMP can go out of the support polygon. One such case is when a sudden stop is commanded while walking at high speed. When this happens, the step position and duration of the current and first step of the next cyclic gait have to be modified as described in [15][16].

The gait pattern generation takes less than 3 ms (PPC G3Gx 1.0GHz) and, on a real robot a new gait pattern is generated at every 5 ms. These fast trajectory generation techniques enable the robot to react robustly against previously unknown obstacles and disturbances.

V. RESULTS

A. Comparison of Boundary Conditions

We compared the proposed boundary condition, the divergent component of motion, against widely used boundary condition, position and velocity. In simulation, a linear inverted pendulum with height of 1000 mm was given a horizontal displacement of 100 mm from the inverted equilibrium. It was then forced to match two different boundary conditions in 350 ms. The first boundary conditions are that it has to rest at the inverted equilibrium, and the other is that the divergent component becomes 0. With the first set of boundary conditions (Fig. 9(a)), the maximum ZMP is 574 mm (e).

For the proposed approach, the pendulum reaches the vertical position after infinite time (b). It can be also observed that the divergent component becomes 0 on time (d) and the convergent component decays to 0 after infinite time (c). The maximum ZMP used is 179 mm (f).

The result shows that the maximum instantaneous ZMP modification is small with the divergent component as the boundary condition instead of position and velocity. The convergence to the equilibrium state over infinite time is also confirmed (c,d) using the divergent component boundary condition.

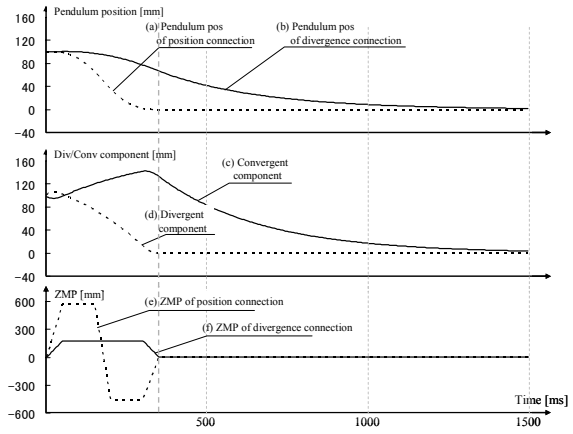

Fig. 9 Divergent component boundary condition

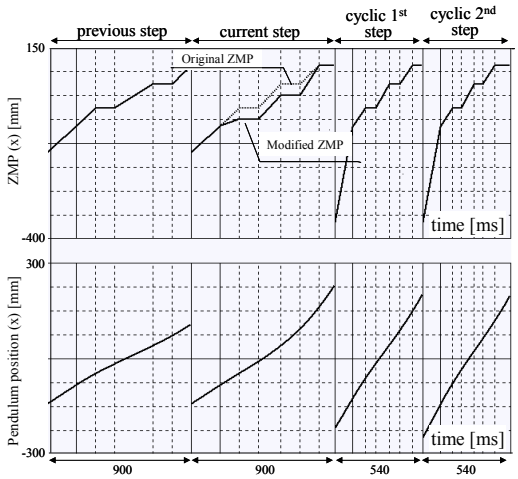

Fig. 10 Acceleration to walking from 1km/h to 3km/h

B. Switching Gait Patterns

We tested the effectiveness of the divergent component using the biped robot shown in Fig. 1. It is 1300 mm tall, weighs 54.0 kg and has six degrees of freedom at each leg. In Fig. 10 is the results of switching from a gait pattern of walking straight at 1.0 km/h with step length of 250 mm and step duration of 900 ms to another gait pattern of walking straight at 3.0 km/h with step length of 450 mm and step duration of 540 ms. The switching was made during the second step.

It can be observed from Fig. 10 that, using the divergent component as the boundary condition, the desired ZMP trajectory is shifted backward to accelerate its body forward. The height of the trapezoid K_{zmp} was -32.22 mm. The result shows that small modification to the ZMP trajectory can achieve sudden switch between two gait patterns without causing the robot to fall.

Fig.11 is another experiment which shows the divergent component, convergent component and the pendulum position. The robot is at rest at the beginning of Fig.11, walks and comes to rest again at the end of the figure. Duration of each step is 550 ms and the instantaneous maximum speed of

this walking is 3.0 km/h. Note that the position of the inverted pendulum is the average of the divergent and convergent components. It can be observed that the divergent component of motion follows the ZMP trajectory as a first order system, and comes to rest on top of it when the robot is at rest. Since we do not actively control the convergent component, it is theoretically possible for it to diverge from ZMP which causes the pendulum to diverge from it as well. This can cause problems with the kinematic constraints of the robot, but we have not seen this behavior for walking up to 4 km/h.

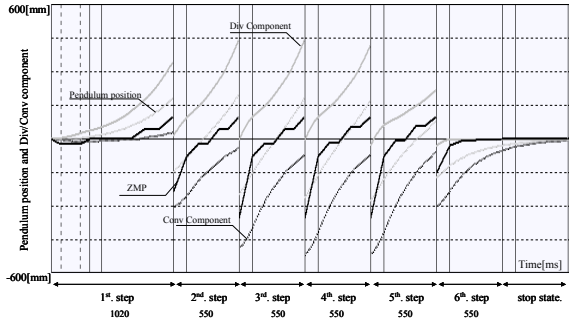

Fig. 11 Divergent and convergent element while walking

C. The Three Mass Model

The moment error around the desired ZMP is transformed to ZMP and shown in Fig.12. The moment error due to approximate dynamics around the desired ZMP was measured for walking at 4.05 km/h with step length of 450 mm and duration of 400 ms. The dynamics error of the proposed model as well as a linear inverted pendulum with a single point mass is computed against a more detailed dynamics model.

During the double support phase, the two approximate dynamics models do not differ by a large margin. But during the single support phase when the robot undergoes large accelerations, the proposed model yields smaller error than the simple pendulum. The standard deviation of the ZMP is 53.5 mm for the proposed model and 29.3 mm for the simple pendulum model.

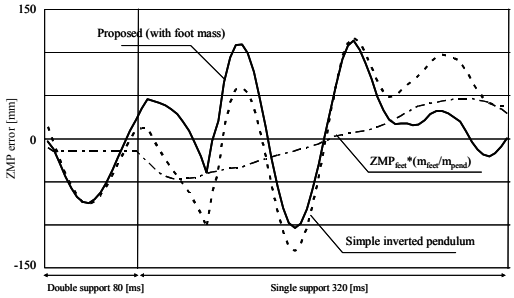

Fig. 12 ZMP error of three mass model and a single mass model

VI. Conclusions

We proposed a dynamics approximation model with three masses for fast generation of gait patterns for biped robots which has small approximation error and computational requirements. We also introduced the concept of divergent and convergent components of motion, and showed that only the divergent component needs to be controlled. Using these techniques, a variety of gait patterns can be generated without having to modify the desired ZMP trajectory largely.

References

[1] K. Hirai, M. Hirose, Y. Haikawa, and T. Takenaka, "The Development of Honda Humanoid Robot", In Proceedings of the 1998 IEEE International Conference on Robotics and Automation, Leuven, Belgium, May. 1998, pp. 1321-1326.

[2] Y. Sakagami, R. Watanabe, C. Aoyama, S. Matsunaga, N. Higaki, and K. Fujimura, "The intelligent ASIMO: System overview and integration", In Proceedings of the 2002 IEEE/RSJ International Conference on Intelligent Robots and Systems, 2002, pp. 2478-2483.

[3] M. Vukobratovi´c and J. Stepanenko, "On the Stability of Anthropomorphic Systems", Mathematical Biosciences, Vol.15, Oct., p.1-37, 1972.

[4] S. Kajita, O. Matsumoto, and M. Saigo, "Real-time 3D Walking Pattern Generation for a Biped Robot with Telescopic Legs", In Proceedings of the 2001 IEEE International Conference on Robotics and Automation, 2001, pp. 2299-2306.

[5] K. Nagasaka, Y. Kuroki, S. Suzuki, Y. Itoh, and J. Yamaguchi, "Integrated Motion Control for Walking, Jumping and Running on a Small Bipedal Entertainment Robot", In Proceedings of the 2004 IEEE International Conference on Robotics and Automation, New Orleans, 2004, pp. 3189-3194.

[6] K. Harada, S. Kajita, K. Kaneko, and H. Hirukawa, "An Analytical Method on Real-time Gait Planning for a Humanoid Robot", Journal of Humanoid Robotics, vol.3, no.1, pp. 1-19, 2006.

[7] T. Sugihara and Y. Nakamura, "A Fast Online Gait Planning with Boundary Condition Relaxation for Humanoid Robots", In Proceedings of the 2005 IEEE International Conference on Robotics and Automation, Barcelona, Apr., 2005, pp. 306-311.

[8] K. Nishiwaki, S. Kagami, Y. Kuniyoshi, M. Inaba, and H. Inoue, "Online Generation of Humanoid Walking Motion based on a Fast generation Method of Motion Pattern that Follows Desired ZMP", In Proceedings of IEEE/RSJ International Conference on Intelligent Robots and Systems, 2002, pp. 2684-2689.

[9] S. Kajita, F. Kanehiro, K. Kaneko, K. Fujiwara, K. Harada, K. Yokoi, and H. Hirukawa, "Biped Walking Pattern Generation by using Preview Control of Zero-Moment Point", In Proceedings of the 2003 IEEE International Conference on Robotics and Automation, 2003, pp. 1620-1626.

[10] J. Yamaguchi, A. Takanishi and I. Kato, "Development of Biped Walking Robot Compensating for Three-Axis Moment by Trunk Motion", In Proceedings of the 1993 IEEE/RSJ International Conference on Intelligent Robot and Systems, 1993, pp. 561-566.

[11] T. Takenaka, T. Matsumoto, T. Yoshiike, and S. Shirokura, "Real Time Motion Generation and Control for Biped Robot -2nd Report: Running Gait Pattern Generation-", In Proceedings of IEEE/RSJ International Conference on Intelligent Robots and Systems, 2009.

[12] T. Takenaka, T. Matsumoto, and T. Yoshiike, "Real Time Motion Generation and Control for Biped Robot -3rd Report: Gait Pattern Modification to Compensate Approximated Dynamics Error-", In Proceedings of IEEE/RSJ International Conference on Intelligent Robots and Systems, 2009.

[13] T. Takenaka, T. Matsumoto, T. Yoshiike, T. Hasegawa, S. Shirokura, H. Kaneko, and A. Orita, "Real Time Motion Generation and Control for Biped Robot -4th Report: Integrated Balance Control-", In Proceedings of IEEE/RSJ International Conference on Intelligent Robots and Systems, 2009.

[14] R.Kurazume,T.Hasegawa and K.Yoneda, “The Sway Compensation Trajectory for a Bipeda Robot”, In Proceedings of the 2003 IEEE International Conference on Robotics and Automations, 2003, pp. 925-931.
[15] T.Sugihara and H.Kobayashi , “A Handy Humanoid Robot Navigation by Non-interruptive Switching of Guided Point and Synergetic Points”, In Proceedings of IEEE/RSJ International Conference on Intelligent Robots and Systems, 2008, pp. 640-645.
[16] M.Morisawa, K.Harada, S. Kajita, K. Kaneko, F. Kanehiro, K.Fujiwara, S.Nakaoka and H. Hirukawa, “A Biped Pattern Generation Allowing Immediate Modification of Foot Placement in Real-time”, IEEE International Conference on Humanoid, 2006, pp. 581-586
[17] R.Tajima, D.Honda and K.Suga, “Fast Running Experiments Involving a Humanoid Robot”, IEEE International Conference on Robotics and Automation, 2008, pp. 1571-1576
[18] S. Kajita, F. Kanehiro, K. Kaneko, K. Fujiwara, K. Harada, K. Yokoi, and H. Hirukawa, “Resolved Momentum Control: Humanoid Motion Planning based on the Linear and Angular Momentum”, In Proceedings of the 2003 IEEE/RSJ International Conference on Intelligent Robots and Systems, Oct. 2003, pp. 1644-1650.
[19] S. Kajita, F. Kanehiro, K. Kaneko, K. Fujiwara, K. Harada, K. Yokoi, and H. Hirukawa, “Biped Walking Pattern Generation by using Preview Control of Zero-Moment Point”, In Proceedings of the 2003 IEEE International Conference on Robotics and Automation, 2003, pp. 1620-1626.
[20] J.H.Park and Kyoung D.Kim, “Biped Robot Walking Using Gravity-Compensated Inverted Pendulum Mode and Computed Torque Control”, In Proceedings of the 1998 IEEE International Conference on Robotics and Automation, 1998, pp. 3528-3533.

APPENDIX

Assume that the ZMP modification pattern in Fig.8 has two degrees of freedom as shown in Fig.13. Using this, it is possible to satisfy two boundary conditions, namely position and velocity or divergent and convergent components of motion. The divergent and convergent components at the end of the phase can be rewritten in terms of the height of each trapezoid, h_1 and h_2, and arbitrary constants $\alpha_1, \alpha_2, \beta_1, \beta_2$.

$$p = \alpha_1 h_1 + \beta_1 h_2$$
$$q = \alpha_2 h_1 + \beta_2 h_2 \quad (25)$$

From Eq. (14), it can be confirmed that both α_1 and β_1 are negative as well as α_2 and β_2. Minimizing the maximum ZMP modification is equivalent to minimizing the following quantity.

$$\max(|h_1|, |h_2|) \quad (26)$$

Fig.13 shows Eq. (25) as two straight lines. The values of which satisfies both of Eq. (25) is the intersection of the two lines marked with a black dot. The point which satisfies only the first of Eq. (25) as well as minimizes Eq. (26) is the intersection of the first equation of (25) and the line $h_1 = h_2$ shown with a white dot. This indicates that the single trapezoid shown in Fig.8 minimizes the maximum modification to the desired ZMP trajectory while satisfying the divergent component constraint. This also implies that adding another constraint such as the convergent component would increase the modification to the desired ZMP

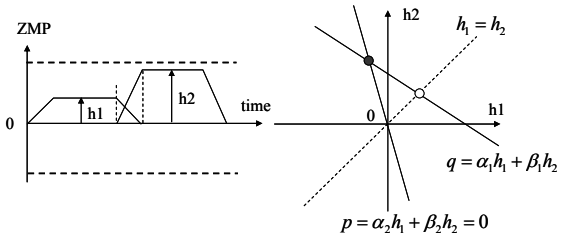

Fig.13 Minimizing ZMP modification pattern height